Soft Matter

www.rsc.org/softmatter

Volume 9 | Number 39 | 21 October 2013 | Pages 9257–9500

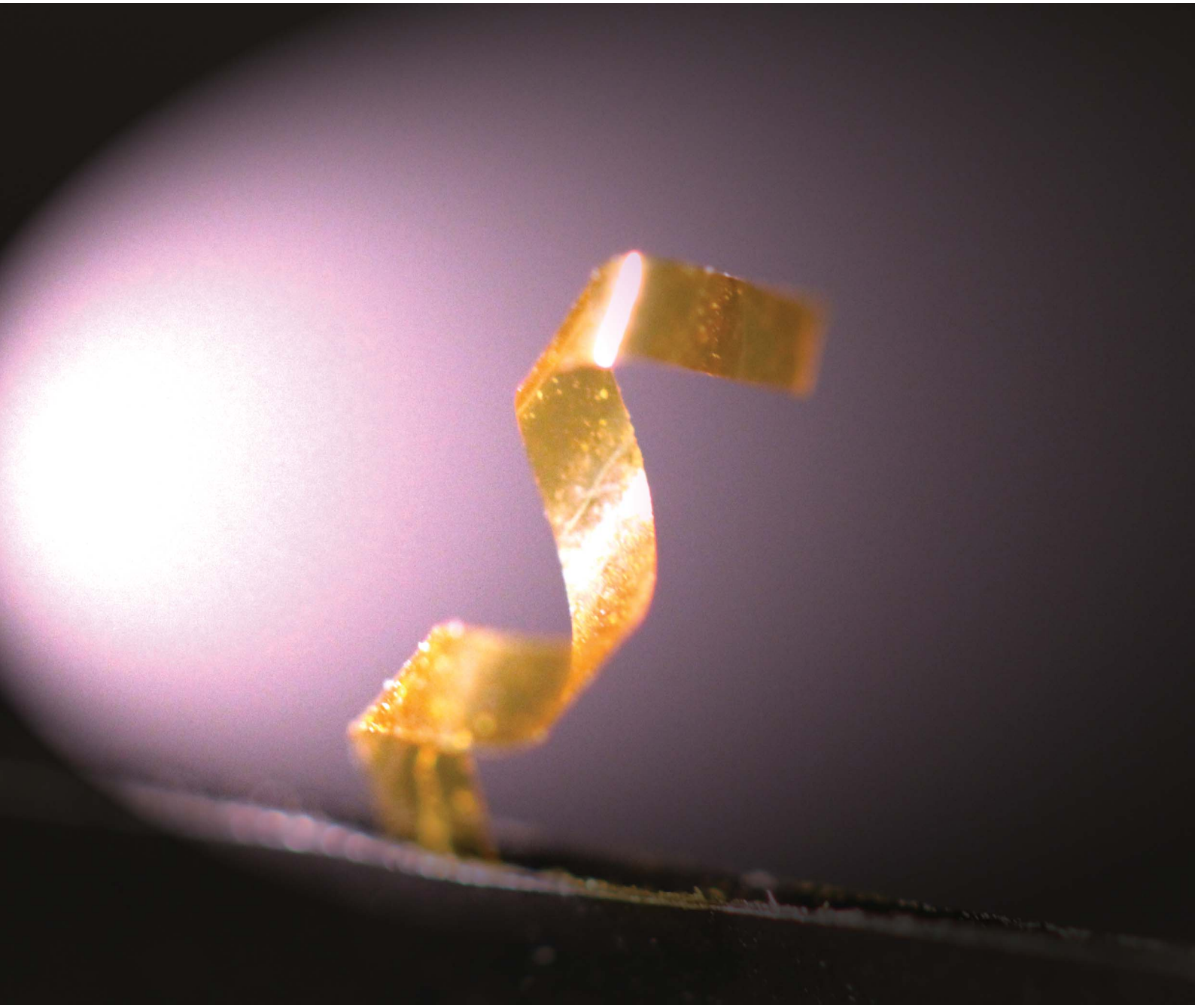

ISSN 1744-683X

RSC Publishing

PAPER

Timothy J. White *et al.*

Torsional mechanical responses in azobenzene functionalized liquid crystalline polymer networks

1744-683X(2013)9:39;1-X

Soft Matter

RSC Publishing

PAPER

View Article Online
View Journal | View Issue

Torsional mechanical responses in azobenzene functionalized liquid crystalline polymer networks†

Cite this: *Soft Matter*, 2013, **9**, 9303

Jeong Jae Wie,[ab] Kyung Min Lee,[ab] Matthew L. Smith,‡[a] Richard A. Vaia[a] and Timothy J. White*[a]

Soft materials capable of both planar and flexural–torsional responses could enable the development of soft robotic elements that emulate the dexterity and functionality of a multitude of creatures in the animal kingdom. Here, we examine the response of azobenzene-functionalized liquid crystal polymer networks (azo-LCNs) specifically focusing on realizing large magnitude flexural–torsional responses observed as out-of-plane twisting or coiling. Towards this end, azo-LCNs were prepared in either the twisted nematic (TN) or hybrid orientations. The characterization of the flexural–torsional photomechanical responses is complimented with examination of thermomechanical properties. The diverse range of tailorable photomechanical responses is shown to be strongly dependent on the alignment of the nematic director to the film geometry and the actinic light intensity.

Received 5th June 2013
Accepted 26th July 2013

DOI: 10.1039/c3sm51574e

www.rsc.org/softmatter

Introduction

Actuators are used to transform an input energy stimulus into motion in order to accomplish tasks requiring mechanical work. Often the force output and functionality of actuators are optimized by integration into mechanical systems (*e.g.*, kinematic linkages).[1] Biological organisms are a daily reminder of the seamless performance enabled by an intricate marriage of sensing (nervous system), structure (skeletal system), and actuation (muscular system). Shape adaptive responses observed in the flex and torsion during the wingbeat[2] or feeding[3] of a hummingbird, the locomotion of a snake,[4,5] or in the throwing motion of a human[6] are vivid illustrations of the capability enabled by coupling actuation and structural design.

Whitesides *et al.* recently published a challenge to the materials community emphasizing the promise of soft material actuation systems in robotics applications.[7] Actuation in soft materials, defined as materials easily deformed by stress, offer large shape deformation, simple processing, and low cost in comparison to hard materials such as shape memory alloys.[8] The materials community has surveyed a variety of stimuli-responsive polymeric materials to transduce input energy into mechanical motion, useful in actuation.[9] Stimuli-responsive polymeric materials have recently been reviewed documenting the applicability in biological interfaces, smart coatings, actuation, and sensing.[10]

Light is a promising input energy stimulus to direct shape adaptive responses in polymeric materials. The work of Lovrien,[11] Agolini,[12] and Eisenbach[13] are foundational to an ever-growing community[14] exploring light-directed mechanical responses in a variety of photoresponsive polymers and composites. Historically, the initial research focused on conventional polymeric morphologies (amorphous, semi-crystalline)[10–12] capable of only small strains (<1%).[14] Within the last ten years, light has been shown to generate considerably larger strain responses in elastomeric liquid crystal polymer networks (LCNs). Accordingly, much of the recent literature on photomechanical effects in polymers has focused on azobenzene-functionalized LCNs (encompassing both glasses and elastomers, referred to here as azo-LCN).[14]

LCNs are polymers composed of mesogenic units, either pendant (side chain) or within (main chain) the polymer backbone. Similar to low-molar mass liquid crystals pervasively employed in the $100B display market, the mesogens within the polymer align into mesophases referred to as the nematic phase (1-d order, orientational) or the smectic phase (2-d order, positional and orientational).[15] Since the original report by Finkelmann,[16] photomechanical deformations in azo-LCNs have been observed as uniaxial contraction of a thin film,[17] polarization-directed bending of a film,[18–20] and reversible bending of a cantilever in a single direction.[21,22] Only recently have out-of-plane deformations been reported.[23,24] The primary chemistries examined to date are siloxane-based azo-LCN elastomers[16,25] and acrylate-based azo-LCN glasses.[18–22,26]

Anisotropic composite materials have been widely utilized to assimilate multiple properties into a single kinematic element

[a]*Air Force Research Laboratory, Materials and Manufacturing Directorate, Wright Patterson Air Force Base, OH, USA. E-mail: Timothy.White.24@us.af.mil; Fax: +1-937-255-1215*

[b]*Azimuth Corporation, 4134 Linden Ave. #300, Dayton, OH 45432, USA*

† Electronic supplementary information (ESI) available: Film geometry effects on photomechanical deformations. See DOI: 10.1039/c3sm51574e

‡ Present address: Hope College, Engineering Department, 27 Graves Place, MI 49423, Holland.

to enable in some cases, multifunctional performance benefits.[27] Layered structures incorporating material anisotropies (or anisotropic input stimuli) have been explored for bistable morphing skins[28] and bending and twisting sensors and actuators made from piezoelectric[29–31] or magnetostrictive materials.[32] A distinct subset of these composites that exhibit a continuous variation of constituent phases are referred to as functionally graded materials (FGM). These materials are currently subject to examination for applications such as prosthetic joints, structural damping, and thermal barrier coatings.[33]

LCNs represent a unique class of self-organized materials that assimilate aspects of both FGM and layered composite actuators. LCNs are monolithic, allowing properties of the material to be varied continuously (similar to FGM) across the film thickness, including in-plane anisotropies. In addition, these materials can be designed to produce large multidimensional deformations and actuated remotely with fine control feasible through local application of the light source. Magnitude, actuation direction, and mode (oscillatory or static) of deformation can be modulated by both polarization and light intensity, giving an unprecedented level of actuator control. Towards this end, this work seeks to further examine the diversity of the planar and flexural–torsional responses realizable in azo-LCN materials in both the twisted nematic and hybrid geometries. The self-organized properties of these polymeric materials enable comparatively large scale deformation to azo-LCNs prepared with conventional nematic (monodomain or polydomain) orientation. Accordingly, large magnitude responses are remotely cued including bending, twisting, and coiling.

Experimental

Synthesis of azobenzene functionalized liquid crystal polymer networks

Azobenzene functionalized liquid crystal polymer networks (azo-LCNs) were synthesized by photopolymerization of a mixture containing 63.5 wt% 4-(3-acryloyloxypropyloxy)-benzoic acid 2-methyl-1,4-phenylene ester ("RM257", Merck), 20 wt% 4,4′-bis[6-(acryoloxy)hexyloxy]azobenzene ("2-azo", BEAM Co.), and 15 wt% 2-propenoic acid, 5-[(4′-cyano[1,1′-biphenyl]-4-yl)-oxy]pentyl ester ("RM23", Merck) with 1.5 wt% of the photoinitiator (Irgacure 784, Ciba). In the preparation of samples with

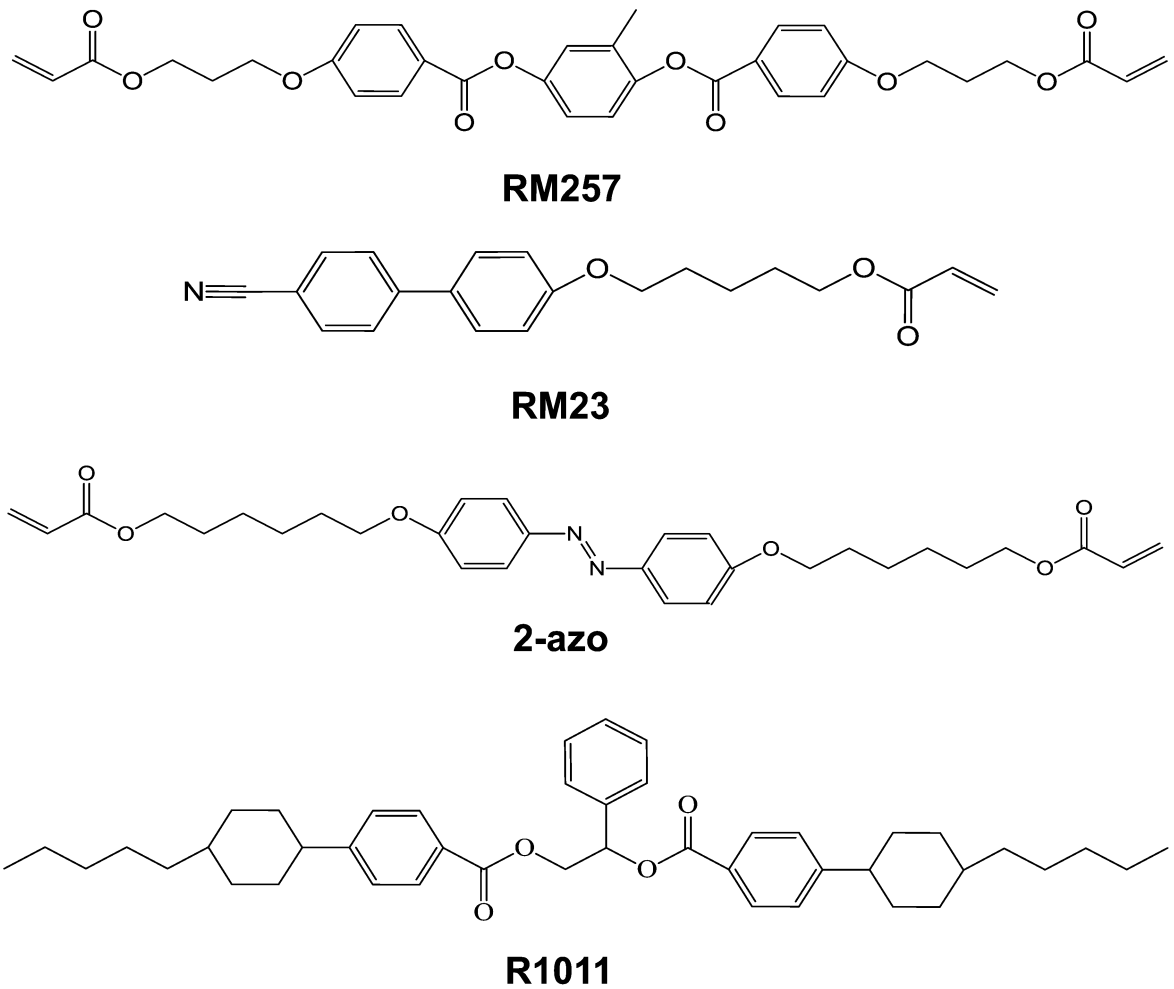

Fig. 1 Chemical structures of the liquid crystal monomers RM257, RM23, 2-azo, and R1011.

the twisted nematic geometry a small amount (0.1 wt%) of chiral dopant ("R1011", Merck) was added (Fig. 1). The 8 μm thick Elvamide-coated twisted nematic or hybrid glass cells (Fig. 2a illustrates twisted nematic and hybrid geometries) were filled with mixtures at 100 °C and subsequently cured by irradiation of 60 mW cm^{-2} of 532 nm light at 75 °C for 1 h.

Characterization methods

The twisted nematic and hybrid geometries of the azo-LCNs were confirmed by polarized optical microscopy (POM, Nikon). Thermomechanical properties of the azo-LCN films were measured by a dynamic mechanical analysis (DMA) (RSA III, TA Instruments) with gauge length of 6 mm (L) × 2 mm (W) × 8 μm (T) in tension. A transient tensile test was conducted with a 0.01 s^{-1} Hencky strain (or true strain) rate to determine the Young's modulus from the initial slope of the stress–strain curves. Glass transition temperature (T_g) was measured at the maximum loss tangent (tan δ) by dynamic temperature step tests with a 2.5 °C min^{-1} of heating ramp and 1 rad s^{-1} of frequency.

Photomechanical responses of the azo-LCN materials were characterized with exposure to the linearly polarized 445 nm laser for 10 min. The polarization direction was controlled by a Fresnel rhomb (Newport) and fixed as parallel to the long axis of the cantilever ($E||x$). The photoinduced deflection of azo-LCN cantilevers was monitored using the film dimension of 6 mm (L) × 0.5 mm (W) × 8 μm (T). The bending angle was calculated from the angle between the mounting point and the tip of cantilever. Subsequent relaxation of the azo-LCN cantilevers was studied by observing the bending angle in the dark.

Results and discussion

The focus of this work is the generation of flexural–torsional mechanical responses in azo-LCN materials prepared with twisted nematic (TN) and hybrid orientations, both of which exhibit a 90° rotation in the director through the sample thickness. As illustrated in Fig. 2a, in the TN geometry the director rotates 90° in the plane of the substrates while in the hybrid geometry the director rotates 90° from planar to homeotropic (normal to substrate). Samples were photopolymerized in

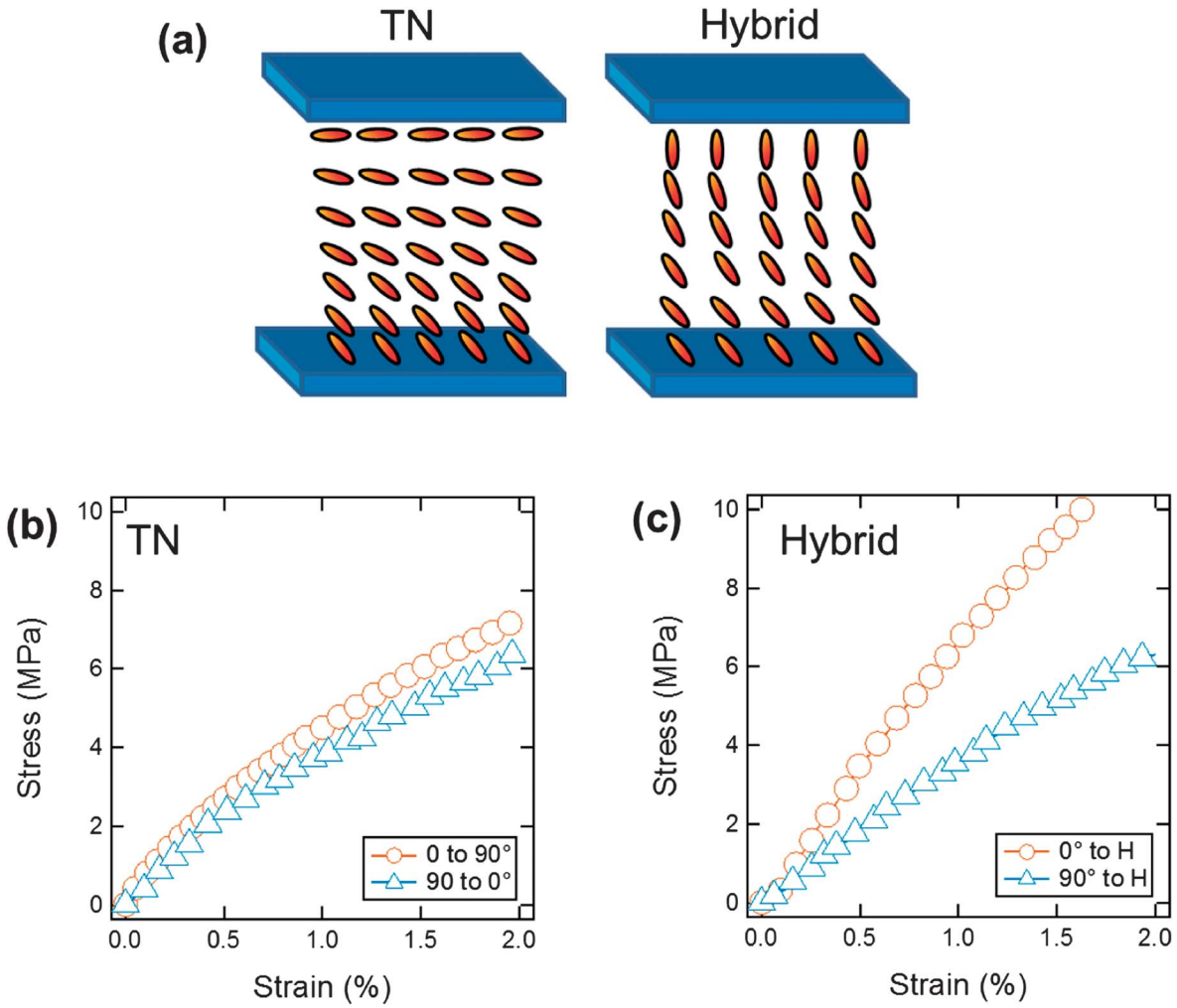

Fig. 2 (a) Illustrations of the twisted nematic (TN) and hybrid geometries of the LCN materials. (b) Mechanical properties measured in films with dimension 6 mm (L) × 0.5 mm (W) × 8 μm (T) for (b) TN and (c) hybrid azo-LCN.

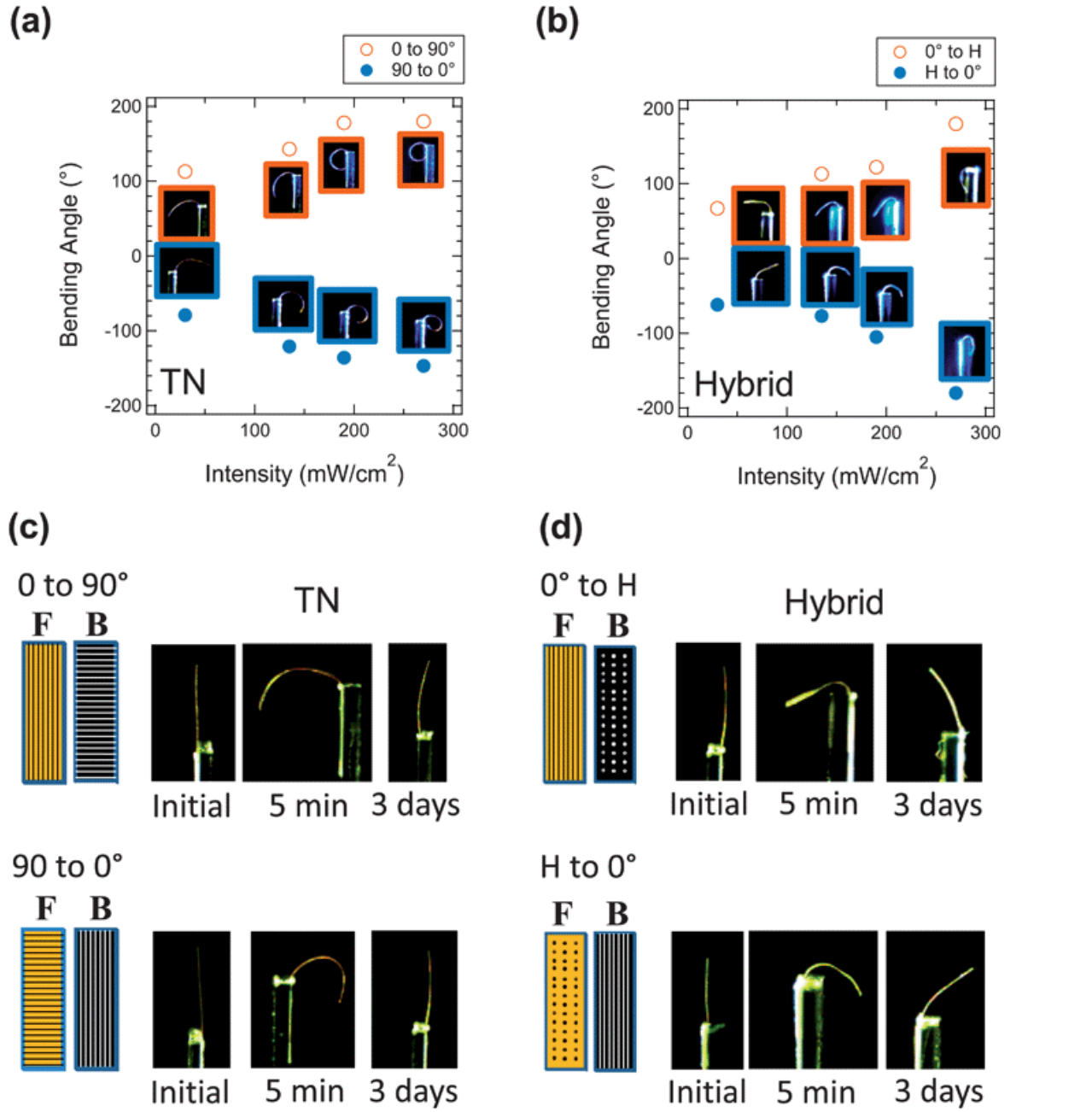

Fig. 3 Photomechanical response of cantilevers composed from TN and hybrid azo-LCN samples. Bending angle of cantilevers composed of (a) TN azo-LCN and (b) hybrid azo-LCN after 10 minutes of exposure to 445 nm laser at intensities ranging from 30 to 270 mW cm^{-2}. (c), (d) Illustration of elastic restoration of TN and hybrid azo-LCN after removal of 445 nm irradiation. All tests employed cantilevers of dimension 6 mm (L) × 0.5 mm (W) × 8 μm (T). F and B indicate front and back surfaces, respectively.

self-prepared liquid crystal alignment cells identical to methods reported previously.[34] In the case of the hybrid geometry, one substrate employed a polyimide rubbing material known to induce homeotropic boundary conditions (PI-2555, HD Micro-Systems) while the other substrate employed a polyamide rubbing material known to induce planar boundary conditions (Elvamide, Du Pont). The TN and hybrid geometries are retained by the azo-LCN material after polymerization. To illustrate the subtle yet important differences in thermomechanical properties, transient stress–strain curves are reported in Fig. 2b (TN) and 2c (hybrid). As expected, the TN sample (Fig. 2b) exhibits largely similar modulus regardless of the alignment of the nematic director to the gauge. Conversely, the apparent modulus of the hybrid azo-LCN materials (Fig. 2c) strongly depends on the alignment of the nematic director to the long axis of the gauge. The glass transition temperatures for the TN and hybrid materials examined here ranged from 35 to 50 °C (taken from the peak of the broad tan δ curves measured by DMA).

The baseline photomechanical response of these materials is summarized in Fig. 3. The photogenerated strain was visualized in the bending of cantilevers of dimension 6 mm × 0.5 mm × 8 μm. Fig. 3a plots the bending angle as a function of light

intensity for cantilevers composed from the TN azo-LCN. Photomechanical responses presented in this work are induced by irradiation with 445 nm light, polarized such that the linear polarization of the light source (E) is parallel to the long axis of the cantilever (x) (referred to as $E\|x$). In all cases, the samples exhibit large magnitude deflections (reported here as bending angle). As evident in Fig. 3a, the directionality of the deflection is governed by the alignment of the nematic director of the TN azo-LCN on the exposed surface of the cantilever. When the nematic director on the exposed surface is parallel to the long axis of the cantilever, light exposure causes bending towards the irradiating source. Conversely, when the nematic director on the front surface is orthogonal to the long axis of the cantilever, light exposure causes bending away from the irradiating source. Such behavior is related to the directionality of the photogenerated strain (extension or contraction on the irradiated surface) to the cantilever geometry and the photochemical mechanism (*trans–cis–trans* reorientation) dictated by the use of 445 nm light. In both of the sample alignment conditions examined in Fig. 3a, increasing the light intensity from 30 to 270 mW cm^{-2} increases the magnitude of the deflection of the cantilever. The photomechanical responses for cantilevers composed of azo-LCN with the hybrid orientation are contrasted in Fig. 3b as a function of actinic light intensity. In both alignment conditions examined in Fig. 3b, the nematic director was aligned parallel to the long axis of the cantilever. However, the directionality of the response is impacted once again by which side of the hybrid sample faces the irradiating light source. When the azo-LCN cantilever is oriented such that the planarly aligned side of the hybrid sample faced the incident light the cantilever deflects towards the light source. However, when the homeotropically aligned side of the hybrid sample faced the incident light the cantilever deflects away from the light source.[35] As with azo-LCN materials prepared with the TN geometry, increasing the intensity of the light exposure to the hybrid azo-LCN samples increases the magnitude of the deflection. The magnitude of the photomechanical deformation of the TN and hybrid azo-LCN materials is considerably larger than monodomain and polydomain azo-LCN materials of identical chemistry. As discussed by Broer and coworkers, these alignment conditions allow for cooperation amongst the front and back surfaces during exposure, which allows for larger deformations.[20] We have previously demonstrated optically-fixable shape memory in polydomain and monodomain azo-LCN materials with similar conditions.[36] As illustrated in Fig. 3c and d, we characterized the shape retention of the photomechanical effects by monitoring the bend angle of the cantilevers for three days after irradiation. Evident in both Fig. 3c and d, the samples retain only a small portion of the photogenerated strain. We hypothesize that the inability of the material to completely retain the bent form in part due to the reduced crosslink density of the material (compared to our prior reports) as well as broad, near-room temperature glass transition temperatures for these materials.

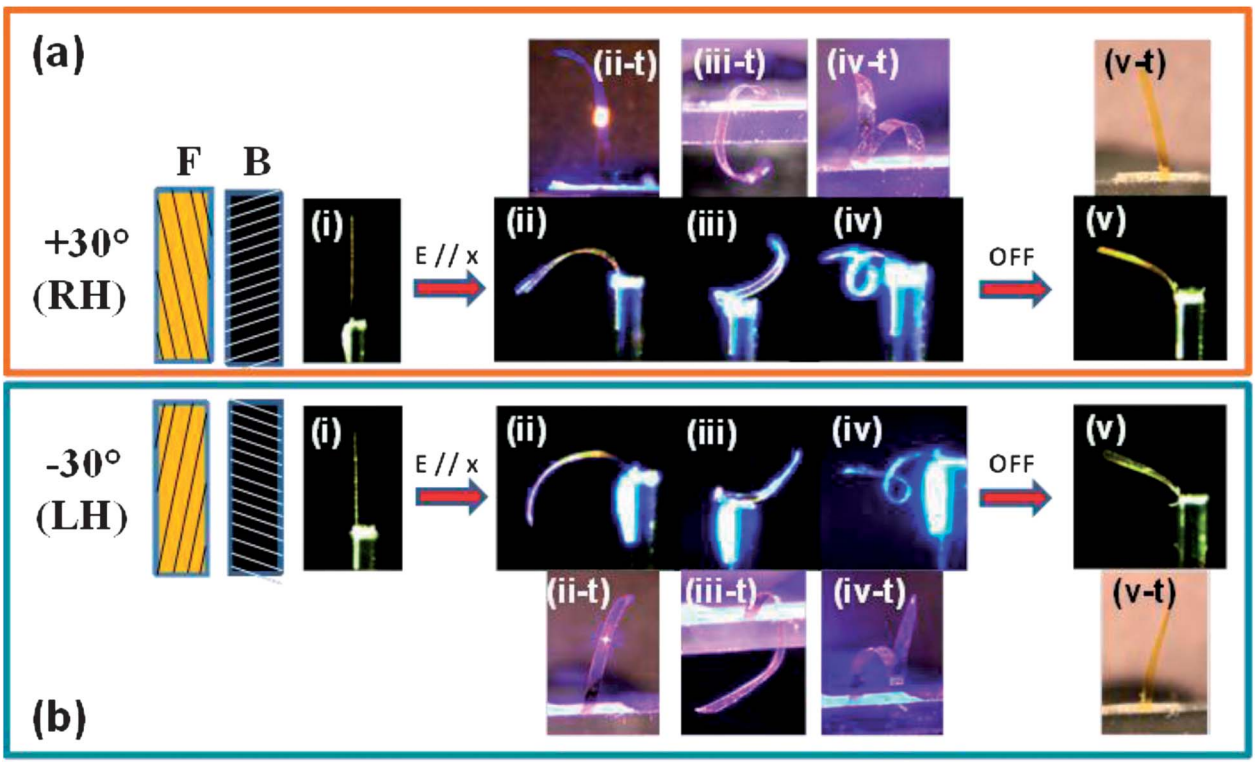

Fig. 4 Flexural–torsional deflection in TN azo-LCN cantilevers. (a) TN azo-LCN samples were cut such that the nematic director on the front surface was (a) +30° and (b) −30°. For both (a) and (b) images are labeled (i)–(v) denoting (i) before exposure, (ii) 30 mW cm^{-2}, (iii) 190 mW cm^{-2}, (iv) 270 mW cm^{-2}, and (v) after 3 days of relaxation. Images marked with (-t) are taken from above. All tests employed cantilevers of dimension 6 mm (L) × 0.5 mm (W) × 8 μm (T).

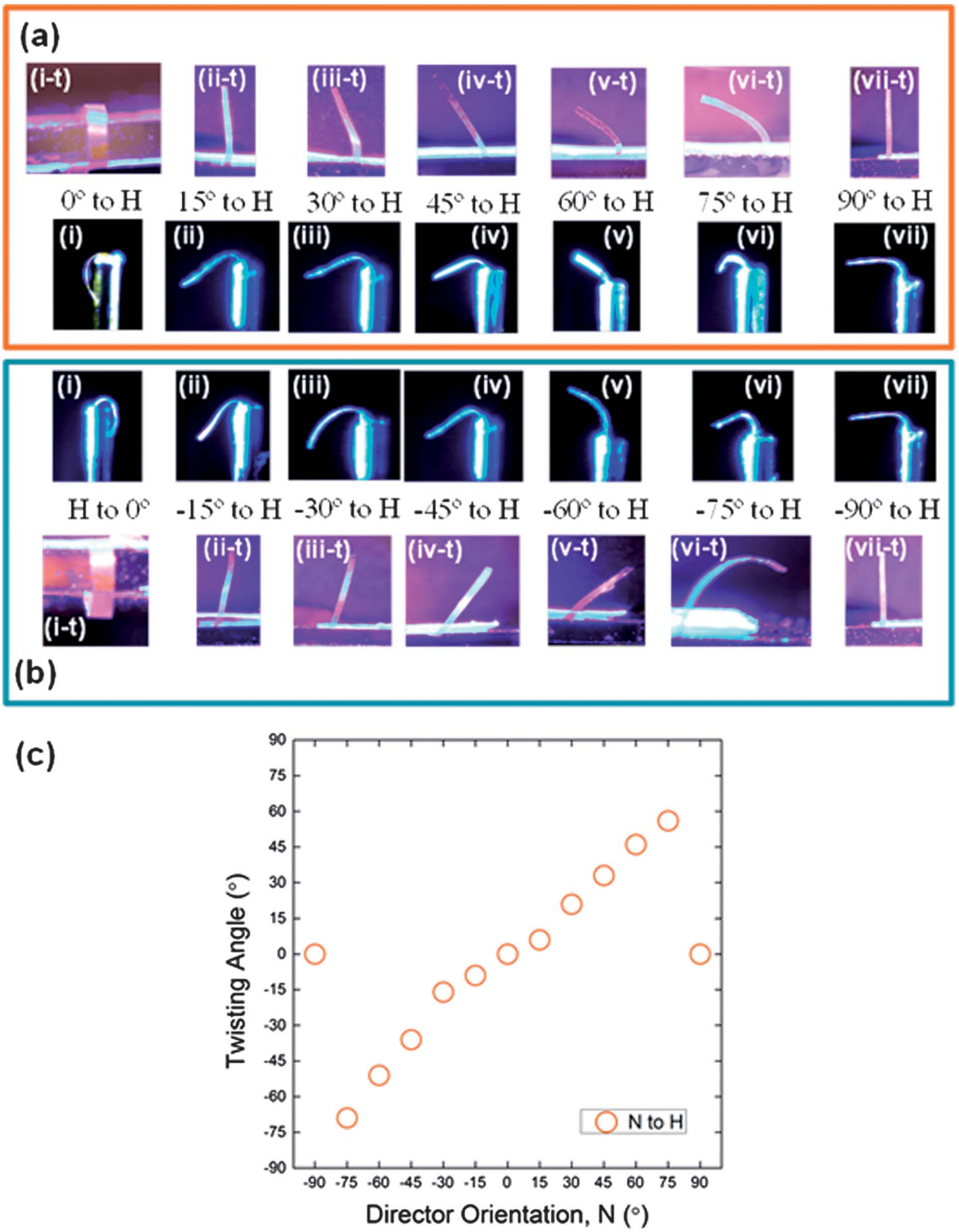

Fig. 5 Deflection to the left (a) or right (b) of cantilevers composed from hybrid azo-LCN when subjected to 270 mW cm^{-2} of 445 nm light for 10 minutes. Images labeled (i → vii) are taken from the side while images labeled (i-t → vii-t) are taken from above. Note, the planarly aligned surface of the hybrid azo-LCN sample was placed on the exposed surface in all samples but that labeled H to 0° in which the homeotropic surface was placed on the exposed surface. (c) Summary of the dependence of out-of-plane twist angle as a function of director orientation of the front surface (homeotropic alignment on back surface).

The ability to wirelessly trigger large magnitude flexural–torsional responses in azo-LCN is shown in Fig. 4. To generate out of plane deformation, the nematic director on the front surface is cut at intermediate angles to the principal axes of the cantilever geometry.[23,24,34] The photomechanical response of cantilevers cut with the nematic director of the TN azo-LCN offset to the principal axes is illustrated in the images in Fig. 4. In Fig. 4a, the nematic director rotates from +30° (front surface, FS) to −60° (back surface, BS) which in Fig. 4b the nematic director rotates from −30° on FS and +60° on the BS. In both alignments, upon irradiation with light the cantilever exhibits both in-plane bending but also out-of-plane twisting. Evident in Fig. 4a, when the TN is aligned such that the FS is +30° and the BS is −60°, the originally flat cantilever (Fig. 4a-i) is deflected downward (Fig. 4a(ii–iv) – view from side) and to the left (Fig. 4a(ii-t–iv-t) – view from top). Evident in the series of images in Fig. 4a(ii–iv), increasing light intensity increases the amount of coiling. When the azo-LCN cantilever is aligned such that that the director is aligned −30° on FS and +60° on the BS 445 nm irradiation with $E\|x$ induces large magnitude in-plane bending (Fig. 4b(ii–iv)) but out-of-plane twisting to the right (Fig. 4b(ii-t–iv-t)). Once again, increasing the intensity of the 445 nm irradiation increases the magnitude of the twisting, resulting in coiling of the cantilever at 190 (Fig. 4b-iii) and 270 mW cm^{-2} (Fig. 4b-iv). Upon removal of the irradiation, the cantilever untwists and returns to a bent state (Fig. 4a-v and b-v). Aligning the nematic director at intermediate angles to the principle axes of the cantilever generates shear.[24] The directionality and magnitude of the photogenerated shear is dominated by the alignment of the director. On the FS, the largest magnitude contraction is occurring along this angle. On the BS, the contraction is offset 90° to this angle. Thus, the photogenerated shear on the FS and BS is cooperative and allows for considerably greater coiling than previous examinations of flexural–torsional deflections in monodomain azo-LCN materials.[24]

Photogenerated, flexural–torsional responses are also observed in azo-LCN samples with the hybrid geometry (Fig. 5). The director profile within the hybrid azo-LCN samples rotates 90°, but from planar to homeotropic across the sample thickness. Thus, cutting hybrid azo-LCN samples in which the nematic director on the exposed surface is offset to the principal axes of the cantilever should also allow for flexural–torsional response. Fig. 5 illustrates the angular selectivity (handedness and magnitude) of the response of the hybrid azo-LCN samples as a function of the angle of the nematic director to the long axis of the cantilever. As evident in Fig. 5, as the angle of the director orientation to the long axis of the cantilever (x) increases from 0°, the magnitude of twisting increases reaching a maximum at ±75° for the angles examined here. As expected, aligning the nematic director ±90° to the front surface of the cantilever results in a planar deflection. As evident in Fig. 5a and b, the handedness of the twisting is governed by the angle of the nematic director to the front surface. When the angle between the nematic director and long axis of the cantilever is negative the samples deflect to the left. When the angle of the nematic director and the long axis of the cantilever is positive the samples deflect to the right. The data in Fig. 5a and b is summarized in Fig. 5c, which plots the magnitude of the out of plane twisting as a function of the alignment of the nematic director to the long axis of the cantilever (x).

Conclusions

In conclusion, light is used to remotely generate large magnitude out-of-plane (flexural–torsional) deformations in azobenzene-functionalized liquid crystal polymer networks (azo-LCN) in both the twisted nematic and hybrid orientation. Offsetting the nematic director of the TN and hybrid azo-LCN materials to the principal axes of the cantilever generates considerable photogenerated shear that can allow the material to coil upon itself. The direction of twisting/coiling is governed by the sign of the angle between the nematic director on the front surface with respect to the long axis of the cantilever.

Acknowledgements

The authors gratefully acknowledge the Materials and Manufacturing Directorate of the Air Force Research Laboratory and the Air Force Office of Scientific Research for financial support. M.L.S. contributed to this work while he held a National Research Council Research Associateship at the Air Force Research Laboratory.

References

1 M. Zupan, M. F. Ashby and N. A. Fleck, *Adv. Eng. Mater.*, 2002, **4**, 933–940.
2 D. R. Warrick, B. W. Tobalske and D. R. Powers, *Nature*, 2005, **435**, 1094–1097.
3 M. L. Smith, G. M. Yanega and A. Ruina, *J. Theor. Biol.*, 2011, **282**, 41–51.
4 D. L. Hu, J. Nirody, T. Scott and M. J. Shelley, *Proc. Natl. Acad. Sci. U. S. A.*, 2009, **106**, 10081–10085.
5 M. Walton, B. C. Jayne and A. F. Bennett, *Science*, 1990, **249**, 524–527.
6 G. S. Fleisig, S. W. Barrentine, N. Zheng, R. F. Escamilla and J. R. Andrews, *J. Biomech.*, 1999, **32**, 1371–1375.
7 F. Ilievski, A. D. Mazzeo, R. E. Shepherd, X. Chen and G. M. Whitesides, *Angew. Chem., Int. Ed.*, 2011, **50**, 1890–1895.
8 C. Liu, H. Qin and P. T. Mather, *J. Mater. Chem.*, 2007, **17**, 1543–1558.
9 T. Mirfakhrai, J. D. W. Madden and R. H. Baughman, *Mater. Today*, 2007, **10**, 30–38.
10 M. A. C. Stuart, W. T. S. Huck, J. Genzer, M. Muller, C. Ober, M. Stamm, G. B. Sukhorukov, I. Szleifer, V. V. Tsukruk, M. Urban, F. Winnik, S. Zauscher, I. Luzinov and S. Minko, *Nat. Mater.*, 2010, **9**, 101–113.
11 R. Lovrien, *Proc. Natl. Acad. Sci. U. S. A.*, 1967, **57**, 236–242.
12 F. Agolini and F. P. Gay, *Macromolecules*, 1970, **3**, 349–351.
13 C. D. Eisenbach, *Polymer*, 1980, **21**, 1175–1179.
14 H. Koerner, T. J. White, N. V. Tabiryan, T. J. Bunning and R. A. Vaia, *Mater. Today*, 2008, **11**, 34–42.

15 M. Warner and E. M. Terentjev, *Liquid Crystal Elastomers,* Oxford University Press, 2003.
16 H. Finkelmann, E. Nishikawa, G. G. Pereira and M. Warner, *Phys. Rev. Lett.*, 2001, **87**, 015501.
17 M. H. Li, P. Keller, B. Li, X. G. Wang and M. Brunet, *Adv. Mater.*, 2003, **15**, 569–572.
18 Y. L. Yu, M. Nakano and T. Ikeda, *Nature*, 2003, **425**, 145.
19 K. D. Harris, R. Cuypers, P. Scheibe, C. L. van Oosten, C. W. M. Bastiaansen, J. Lub and D. J. Broer, *J. Mater. Chem.*, 2005, **15**, 5043–5048.
20 C. L. van Oosten, K. D. Harris, C. W. M. Bastiaansen and D. J. Broer, *Eur. Phys. J. E: Soft Matter Biol. Phys.*, 2007, **23**, 329–336.
21 T. J. White, S. V. Serak, N. V. Tabiryan, R. A. Vaia and T. J. Bunning, *J. Mater. Chem.*, 2009, **19**, 1080–1085.
22 K. M. Lee, H. Koerner, R. A. Vaia, T. J. Bunning and T. J. White, *Macromolecules*, 2010, **43**, 8185–8190.
23 Y. Sawa, F. F. Ye, K. Urayama, T. Takigawa, V. Gimenez-Pinto, R. L. B. Selinger and J. V. Selinger, *Proc. Natl. Acad. Sci. U. S. A.*, 2011, **108**, 6364–6368.
24 K. M. Lee, M. L. Smith, H. Koerner, N. Tabiryan, R. A. Vaia, T. J. Bunning and T. J. White, *Adv. Funct. Mater.*, 2011, **21**, 2913–2918.
25 P. M. Hogan, A. R. Tajbakhsh and E. M. Terentjev, *Phys. Rev. E: Stat., Nonlinear, Soft Matter Phys.*, 2002, **65**, 041720.
26 C. L. van Oosten, D. Corbett, D. Davies, M. Warner, C. W. M. Bastiaansen and D. J. Broer, *Macromolecules*, 2008, **41**, 8592–8596.
27 R. F. Gibson, *Compos. Struct.*, 2010, **92**, 2793–2810.
28 C. Thill, J. Etches, I. Bond, K. Potter and P. Weaver, *Aeronaut. J.*, 2008, **112**, 117–139.
29 P. Muralt, R. G. Polcawich and S. Trolier-McKinstry, *MRS Bull.*, 2009, **34**, 658–664.
30 H. Kioua and S. Mirza, *Smart Mater. Struct.*, 2000, **9**, 476–484.
31 A. A. Bent, N. W. Hagood and J. P. Rodgers, *J. Intell. Mater. Syst. Struct.*, 1995, **6**, 338–349.
32 V. H. Guerrero and R. C. Wetherhold, *J. Magn. Magn. Mater.*, 2004, **279**, 343–352.
33 V. Birman and L. W. Byrd, *Appl. Mech. Rev.*, 2007, **60**, 195–216.
34 K. M. Lee, T. J. Bunning and T. J. White, *Adv. Mater.*, 2012, **24**, 2839–2843.
35 M. Kondo, J. Mamiya, M. Kinoshita, T. Ikeda and Y. L. Yu, *Mol. Cryst. Liq. Cryst.*, 2007, **478**, 1001–1013.
36 K. M. Lee, H. Koerner, R. A. Vaia, T. J. Bunning and T. J. White, *Soft Matter*, 2011, **7**, 4318–4324.